

Research Article

Maximum Power Point Tracking Control of PV-TE Hybrid Power Generation System in Greenhouse

Long Bai 

School of Physics and Electronic Engineering, Mudanjiang Normal University, Mudanjiang 157011, Heilongjiang, China

Correspondence should be addressed to Long Bai; 0902017@mdjnu.edu.cn

Received 18 May 2022; Accepted 23 June 2022; Published 31 July 2022

Academic Editor: Zaoli Yang

Copyright © 2022 Long Bai. This is an open access article distributed under the Creative Commons Attribution License, which permits unrestricted use, distribution, and reproduction in any medium, provided the original work is properly cited.

The application of photovoltaic-thermoelectric (PV-TE) combined power generation system in greenhouse is an effective way to solve the problems of high energy consumption and high pollution. In order to improve the efficiency of the PV-TE system, maximum power point tracking (MPPT) control is required. Aiming at the shortcomings of the traditional incremental conductance (INC) method, which is fixed in step size, a hyperbolic tangent-type adaptive variable step length INC method is proposed. The method takes advantage of the monotonically increasing and the fast changing speed of the hyperbolic tangent function, so that the step length can be adjusted rapidly and adaptively according to the change of external environmental conditions such as light intensity. The simulation results show that the proposed method can rapidly track the maximum power point when the illumination intensity changes drastically, and meanwhile it has smaller steady-state error and can realize MPPT control well.

1. Introduction

The development and progress of science and technology have promoted the gradual popularization of the new type of greenhouse under the concept of “Internet +.” With the increase of sensors and other devices in the greenhouse, the disadvantages of complex installation, inconvenient maintenance, and low performance-to-price ratio of traditional power supply mode are becoming more and more obvious, and people pay more and more attention to the environmentally friendly and convenient solar energy [1, 2]. However, the power generation efficiency of photovoltaic cells will decrease greatly with the increase of working temperature in order to solve this problem. Vorobiev et al. [3] proposed photovoltaic-thermoelectric power generation technology, which uses the excess heat generated by photovoltaic cells as the heat source of thermoelectric power generation system to achieve secondary power generation, so as to improve the power generation efficiency of the whole system. However, in practical use, it is necessary for the photovoltaic/thermoelectric power generation system to work at the maximum power point as far as possible to maximize the potential of the system.

At present, there are few literature on the maximum power point tracking control of photovoltaic-thermoelectric

power generation system, and the control method of photovoltaic power generation system is mainly borrowed. The commonly used methods include constant voltage method [4] (CV), disturbance observation method [5] (perturbation and observation method, P&O), and incremental conductance method [6] (INC). In addition, some intelligent heuristic algorithms are also applied to maximum power point tracking control, such as fuzzy control [4], artificial neural network [7], and particle swarm optimization algorithm [8]. Among them, the conductance increment method is simple in principle and easy to implement, and it is a method that can truly realize maximum power point tracking control in theory. However, this method also has obvious defects, that is, the use of fixed step size, and improper selection will lead to the algorithm and cannot find the maximum power point or oscillation in time. In order to solve this problem, a conductance increment method based on model reference is proposed in reference [9]. Firstly, the maximum power points with different light intensity and temperature are found as the reference model under the condition of simulation. Then in practical use, the conductance increment method is used to find the real maximum power points near these points. Although the simulation results show that this method can

effectively improve the tracking accuracy of the maximum power point, the establishment of the previous reference model needs to consider too many parameters. Literature [10] combines the particle swarm optimization algorithm with the conductance increment method. Firstly, the particle swarm optimization algorithm is used to predict the voltage and current near the maximum power point, and then the conductance increment method is used to find the maximum power point according to these two values, and a good tracking effect is achieved. However, this method has high computational complexity and high hardware cost. Literature [11] combines the constant voltage method with the conductance increment method and uses the constant voltage method to quickly locate near the maximum power point in the initial stage. Then, the conductance increment method is used to find the maximum power point, and the step size can be changed dynamically by changing the scale factor K . However, this method only uses the maximum step size in the traditional conductance increment method to simply limit the scale factor and does not really realize self-adaptation. The same control strategy is adopted in reference [12]. The difference is that the scale factor K is given by trial and error method, so this method has poor flexibility and robustness. In reference [13], an adaptive conductance increment method is proposed, which can automatically adjust the step size according to the changes of the external environment. A new step size adjustment coefficient is adopted to improve the response speed of the algorithm. However, the essence of this method is the same as that of references [11, 12], only the form of step size adjustment factor has changed slightly, and it is still unable to achieve real self-adaptation.

Based on the above analysis, in order to better realize the maximum power point tracking control of the photovoltaic-temperature difference combined power generation system, an adaptive variable step size conductance increment method is proposed to solve the problems of oscillation and misjudgment in the simple conductance increment method. This method makes use of the characteristics of the hyperbolic tangent function, so that the step size of the conductance increment method can be changed adaptively, and the tracking speed and steady-state characteristics of the algorithm are effectively improved. The MATLAB/Simulink simulation results show that the adaptive conductance increment method not only has faster tracking speed than the traditional conductance increment method, but also has smaller steady-state output power fluctuation, stronger robustness to external environment disturbance, and higher energy utilization.

2. Photovoltaic-Temperature Difference Combined Power Generation System

2.1. System Structure and Principle. The structure of the photovoltaic-thermoelectric power generation system is shown in Figure 1. The photovoltaic cell and the high temperature end of the thermoelectric chip are connected by high thermal conductivity insulating silica gel, while the low temperature end of the thermoelectric chip is connected with the cooling system by a high thermal conductivity

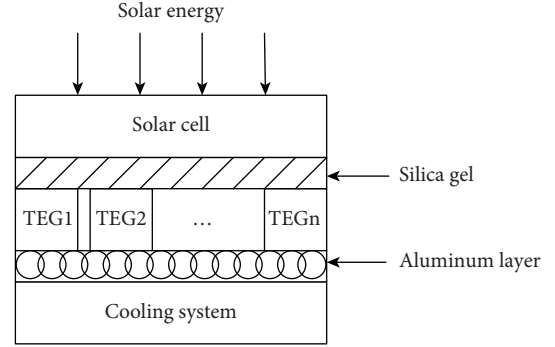


FIGURE 1: Structure of photovoltaic-thermoelectric power generation system.

aluminum layer. In traditional photovoltaic power generation systems, the heat caused by sufficient light in photovoltaic power generation will hinder the photovoltaic effect and reduce the photovoltaic power generation efficiency. Usually, when the crystal silicon cell temperature increases by 1°C , the photovoltaic conversion efficiency will be reduced by 3% to 5%. Too high temperature will also shorten the working life of photovoltaic cells [14]. The combined photovoltaic-thermoelectric power generation technology takes the heat that affects the conversion efficiency and working life of photovoltaic cells as the heat source of thermoelectric power generation, and converts the waste heat of photovoltaic cells into electric energy through thermoelectric cells, thus realizing the secondary utilization of solar energy. The output efficiency of the system is improved.

2.2. Mathematical Model of the System. Solar energy cannot be completely absorbed by photovoltaic cells, some of which will be released into the environment in the form of heat transfer, convection, or radiation. Because the heat loss follows Newtonian linear heat transfer law and radiation heat transfer law, the heat balance equation of photovoltaic cell surface can be obtained from the law of conservation of energy [15].

$$GA_{PV} = Q_{in} + \varepsilon\delta A_{PV}(T_P^4 - T_a^4) + hA_{PV}(T_P - T_a). \quad (1)$$

Among them, G represents the intensity of solar radiation, A_{PV} represents the area of the battery panel, Q_{in} indicates the amount of heat absorbed by the battery (per unit time), ε and h represent the reflectivity and heat transfer coefficient (unit area) of the panel, δ is the Boltzmann constant, and T_P and T_a represent the surface temperature and ambient temperature of the panel, respectively.

The Newtonian heat transfer law is also obeyed between the photovoltaic cell and the thermoelectric chip, so the Q_{in} of the energy absorbed by the thermoelectric chip per unit time from the photovoltaic cell is

$$Q_P = Q_{in} - P_{PV} = U_h A_h (T_P - T_H). \quad (2)$$

Among them, P_{PV} is the power output of photovoltaic cells, U_h is the thermal conductivity, A_h is the heat exchange

area, and T_h is the hot end temperature of the thermoelectric sheet.

Formula (1) and type (2) are available:

$$\begin{aligned} A_{PV} \left[G - \varepsilon \delta (T_p^4 - T_a^4) - h(T_p - T_a) \right] - I_{PV}^2 R_{L1} \\ - U_h A_h (T_p - T_H) = 0. \end{aligned} \quad (3)$$

Some of the heat absorbed by the thermoelectric plates will also be lost to the environment:

$$Q_{\text{loss}} = K_0 (T_H - T_a). \quad (4)$$

Among them, K_0 is the thermal conductivity between the thermoelectric sheet and the environment.

According to the first law of thermodynamics, the final heat absorbed by the thermoelectric sheet is

$$Q_H = Q_{\text{in}} - P_{PV} - Q_{\text{loss}}. \quad (5)$$

According to the characteristics of the thermoelectric sheet, Q_h can be obtained as follows:

$$Q_H = \frac{\alpha^2 T_H (T_H - T_C)}{R_i + R_{L2}} + k(T_H - T_C) - \frac{1}{2} \frac{\alpha^2 R_i (T_H - T_C)}{R_i + R_{L2}}. \quad (6)$$

where k is the heat conduction coefficient between the hot end and the cold end of the thermoelectric sheet. Formulas (5) and (6) can be obtained:

$$\begin{aligned} \frac{\alpha^2 T_H (T_H - T_C)}{R_i + R_{L2}} + k(T_H - T_C) - \frac{1}{2} \frac{\alpha^2 R_i (T_H - T_C)}{R_i + R_{L2}} \\ - A_{PV} \left[G - \varepsilon \delta (T_p^4 - T_a^4) - h(T_p - T_a) \right] + I_{PV}^2 R_{L1} \\ + K_0 (T_H - T_a) = 0. \end{aligned} \quad (7)$$

According to formulas (3) and (7), the working temperature T_p of the photovoltaic cell and the hot end temperature T_H of the thermoelectric chip can be obtained by setting different loads of R_{L1} and R_{L2} .

In the process of transferring heat to the cooling system, due to the high thermal conductivity of aluminum, there is little heat dissipated into the environment. Ignoring this part of the loss, the heat absorbed by the cooling system is as follows:

$$Q_C = mc(T_{co} - T_{ci}), \quad (8)$$

where m is the mass flow rate of water flowing through the cooling system (kg/s) per unit time, c is the specific heat of water, T_{co} is the outlet temperature of the cooling system, and T_{ci} is the inlet temperature of the cooling system (default is 0).

And because of the temperature difference, the heat Q_c of the cold end of the generator is

$$Q_C = \frac{\alpha^2 T_C (T_H - T_C)}{R_i + R_{L2}} + k(T_H - T_C) - \frac{1}{2} \frac{\alpha^2 R_i (T_H - T_C)}{R_i + R_{L2}}. \quad (9)$$

Therefore, the outlet temperature of the cooling system is

$$\begin{aligned} T_{co} &= \frac{Q_C}{mc} \\ &= \frac{\alpha^2 T_C (T_H - T_C) / R_i + R_{L2} + k(T_H - T_C) - 1/2 \alpha^2 R_i (T_H - T_C) / R_i + R_{L2}}{mc}, \end{aligned} \quad (10)$$

T_p , T_H , and T_{co} are three very important parameters for the photovoltaic-thermoelectric combined power generation system, which can affect the overall power generation performance of the system.

From the above heat conversion process, it can be seen that the electricity output of the photovoltaic cell and the thermoelectric chip in the combined system is relatively independent, so the overall output power and power generation efficiency of the system can be obtained immediately by combining the two mathematical models:

$$\begin{aligned} P &= P_{PV} + NP_{TE} = I_{PV}^2 R_{L1} + NI_{TE}^2 R_{L2}, \\ \eta &= \frac{P}{GA_{PV}} = \frac{I_{PV}^2 R_{L1} + NI_{TE}^2 R_{L2}}{GA_{PV}}, \end{aligned} \quad (11)$$

where N is the number of thermoelectric plates.

3. Adaptive Variable Step Size MPPT Control

At the beginning of the birth of the conductance increment method, because the performance of the algorithm is very dependent on the accuracy and speed of voltage and current detection, it is rarely used. However, with the rapid development of microelectronics, integrated circuits, and sensing technology, a large number of high-speed, high-precision digital-to-analog converters, and high-performance DSP appear, which makes it possible to popularize the application of conductance increment method. The conventional conductance increment method mostly uses the fixed step size method for maximum power point tracking, but this fixed step size conductance increment method has obvious defects: if the step size is too small, it will make the photovoltaic cell stay in the low power output region for a long time; if the step size is too large, it will aggravate the oscillation.

3.1. The Basic Principle of Conductance Increment Method.

Figure 2 shows the output characteristic curve of the photovoltaic-temperature difference combined power generation system under different temperatures and different light conditions. It can be seen from the figure that the voltage-power curve is a unimodal curve, so there must be a unique maximum power point, which makes $dP/dU = 0$. Then, the relationship between power and voltage and current can be obtained:

$$\frac{dP}{dU} > 0 = \frac{d(UI)}{dU} = I + U \frac{dI}{dU}. \quad (12)$$

Since there is only one maximum power point U_{max} , it can be considered in three cases:

- ① $dP/dU > 0$, $dI/dU > -I/U$. At this point, the power point is U_{max} on the left, $U < U_{\text{max}}$

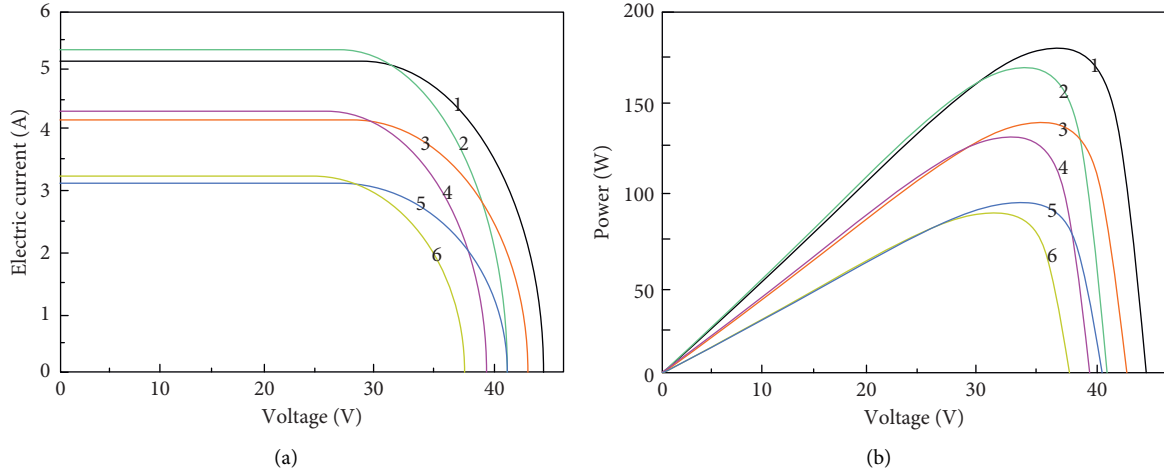


FIGURE 2: Output characteristics of the system under a different temperature and light. (a) Voltage-current characteristic curve. (b) Voltage-power characteristic curve.

- ② $dP/dU < 0$, $dI/dU < -I/U$. At this time, the power point is on the right side of U_{\max} , $U > U_{\max}$
- ③ $dP/dU = 0$, $dI/dU = -I/U$. At this point, the power point is U_{\max} , $U = U_{\max}$

Thus, it can be seen that whether the current power point is the maximum power point can be judged by comparing the relationship between dP/dU and $-I/U$. If it is case 1, then

$$U_{\text{ref}} = U + \Delta U. \quad (13)$$

If it is case 2, then

$$U_{\text{ref}} = U - \Delta U. \quad (14)$$

The obvious defect of the conductance increment method is that the step size ΔU is fixed and needs to be given by experience or trial and error method. Improper selection will have a great impact on the performance of the algorithm. If ΔU is too large, the tracking performance of the maximum power point is better, but there is a serious oscillation phenomenon, and the steady-state error is larger; on the contrary, if ΔU is too small, the oscillation phenomenon is weakened, but the tracking speed will become slower. Therefore, the effect of fixed step size conductance increment method is not good in practice.

3.2. Adaptive Variable Step Size Conductance Increment Method. Considering the defects of the conventional conductance increment method, a natural improvement idea is to adjust the step size dynamically. When the output power of the system is far away from the maximum power point, the step size should be set larger to speed up the dynamic response of the system; when the output power of the system is close to the maximum power point, the step size will reduce the steady-state error of the system and prevent the system from oscillating. From the basic principle of conductance increment method, it is known that there is a strong relationship between step size change and dP/dU , so dP/dU can be used as a coefficient of step size adjustment.

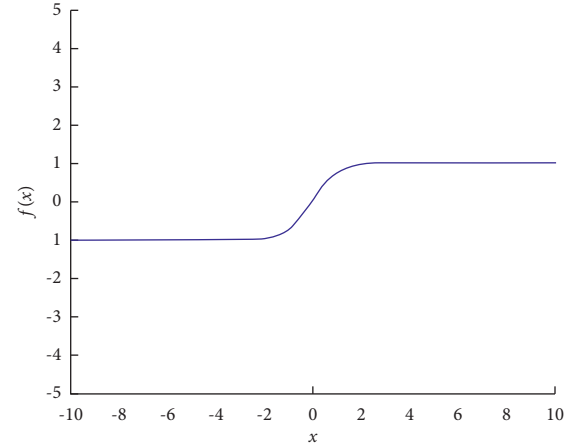


FIGURE 3: Characteristics of hyperbolic tangent function.

Define the following hyperbolic tangent function:

$$f(x) = \frac{e^x - e^{-x}}{e^x + e^{-x}}. \quad (15)$$

Its characteristic curve is shown in Figure 3.

It can be seen from Figure 3 that the hyperbolic tangent function is a monotone increasing function, and the value range of $f(x)$ is $[-1, 1]$, and when $x \in [-\infty, -2]$ and $x \in [2, \infty]$, $f(x)$ almost takes a positive or negative maximum, while when $x \in [-2, 2]$, x changes rapidly in a monotone increasing manner. This is completely consistent with the expected step size change, so consider dI/dU as the function-independent variable and step ΔU as the function variable. In addition, from a great deal of practical experience, it is known that there is generally a maximum ΔU_{\max} set by the fixed step size conductance increment method, and the step size of the variable step size conductance increment method should not exceed this value. Considering these factors, the adaptive adjustment formula of step size proposed in this paper is

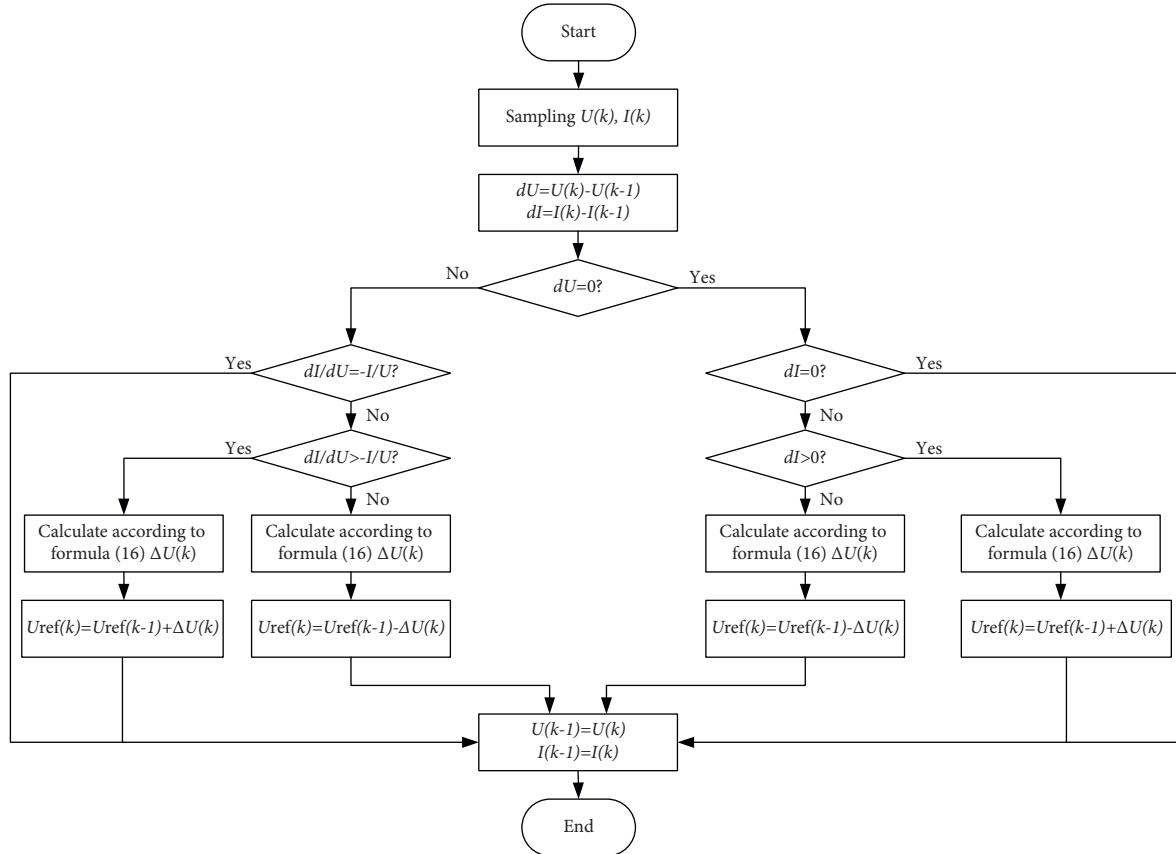


FIGURE 4: Implementation flow of adaptive variable step size conductance increment method.

$$\Delta U(k) = \Delta U_{\max} \frac{e^{dI(k)/dU(k)} - e^{-dI(k)/dU(k)}}{e^{dI(k)/dU(k)} + e^{-dI(k)/dU(k)}}. \quad (16)$$

In this way, when the output power of the system is far away from the maximum power point, the maximum step size is almost adjusted, and when the output power is close to the maximum power point, the step size can be quickly reduced, so that the tracking characteristics and steady-state error of the system can achieve good results at the same time.

The implementation flow of the adaptive variable step size conductance increment method is shown in Figure 4.

4. Experimental Analysis Program

In order to test the performance of the adaptive variable step size conductance increment method in the maximum power point tracking control of photovoltaic-thermoelectric combined power generation system, the algorithm is simulated by MATLAB/Simulink software. The DC-DC circuit is in the form of boost, and the circuit structure is shown in Figure 5. The simulation structure of photovoltaic-thermoelectric power generation is shown in Figure 6.

The photovoltaic cell simulation model used in this paper is the JAMG-6-60-250/SI photovoltaic module of Jingao Company, and some of its main parameters are shown in Table 1. The simulation model of thermoelectric chip is F40550 of Xinghe Company, and some of its main parameters are shown in Table 2 [16].

The most important thing to evaluate the MPPT algorithm is to verify the tracking performance of its maximum power point. In the experiment, the light intensity changed from 400 W/m^2 to 1000 W/m^2 at 0.1 s and back to 400 W/m^2 at 0.2 s. In order to evaluate the performance of the algorithm more objectively, the proposed algorithm is compared with the traditional fixed step size conductance increment method and the variable step size conductance increment method proposed in reference [13]. The results are shown in Figure 7. Among them, the fixed step size conductance increment method selects two kinds of step size, which are smaller $\Delta U = 0.1$ and larger $\Delta U = 0.5$, and the maximum change value of step size in literature [13], and this algorithm is also set to 0.5 [17]–[19].

As can be seen from Figure 7, the variable step size conductance increment method proposed in this paper has the best tracking performance. Specifically, for the fixed step size conductance increment method, when the illumination suddenly increases, the system adjustment time of small step and large step is 46.3 ms and 24.2 ms, respectively; when the illumination suddenly decreases, the system adjustment time is 34.8 ms and 13.5 ms, respectively; when the light intensity is stable, the average output power of the system is 317.4 W and 324.7 W, respectively. It can be seen that when the step size is larger, the start-up speed and dynamic response time of the algorithm are obviously better, but the corresponding steady-state error is larger and the output power oscillation is obvious, which leads to the decrease of the overall efficiency of the system.

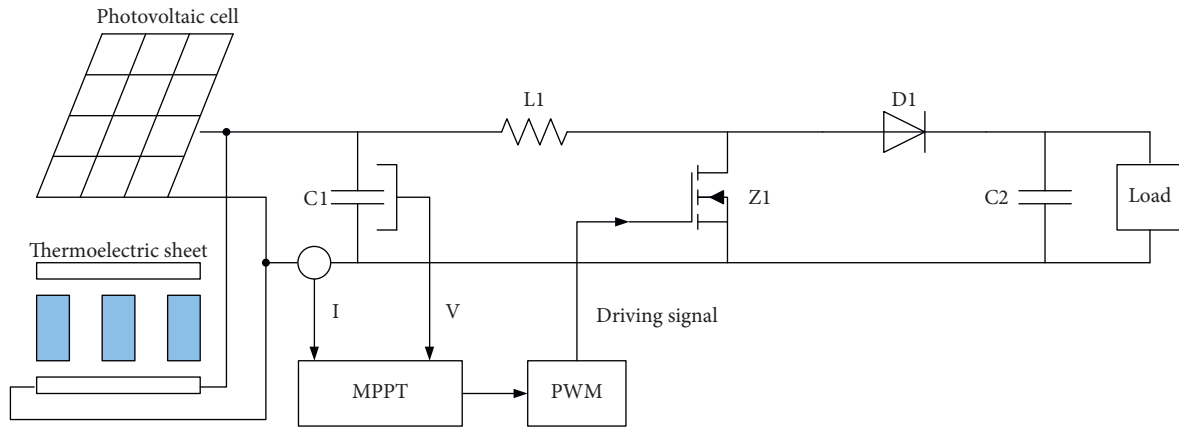


FIGURE 5: Simulation circuit structure.

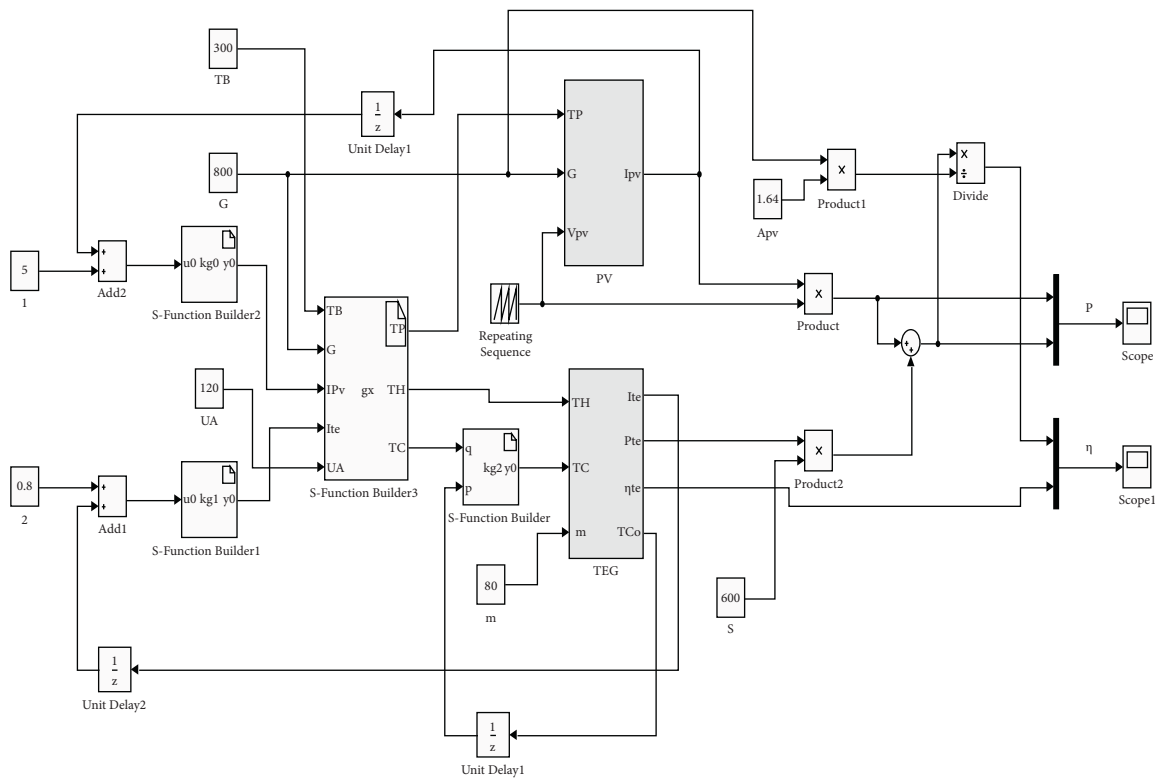


FIGURE 6: Simulation block diagram of photovoltaic-temperature difference system.

TABLE 1: Main parameters of photovoltaic cells.

PV parameters	Values
Short-circuit current I_{sc}/A	8.62
Open-circuit voltage V_{oc}/V	37.92
Temperature coefficient of $I_{sc}/(\% \cdot ^\circ C^{-1})$	0.04
Temperature coefficient of $V_{oc}/(\% \cdot ^\circ C^{-1})$	-0.3
Maximum power/W	250

TABLE 2: Main parameters of thermoelectric generator.

TEG parameters	Temperature difference/ $^\circ C$		
	20	40	60
Open-circuit voltage V_{oc}/V	32	55	81.8
Maximum voltage V_{max}/V	15	25.2	36.8
Maximum current I_{max}/A	4.47	7.59	11.7
Maximum power/W	66.0	198	408

The performance of the algorithm in reference [13] is obviously better than that of the fixed step size conductance increment method. The average output power of the system is 317.8 W when the light intensity is 1000 W/m^2 , which

shows that the algorithm can improve the tracking speed and steady-state accuracy of the system to a certain extent.

The adjusting time of the variable step size conductance increment method proposed in this paper is 12.5 ms and

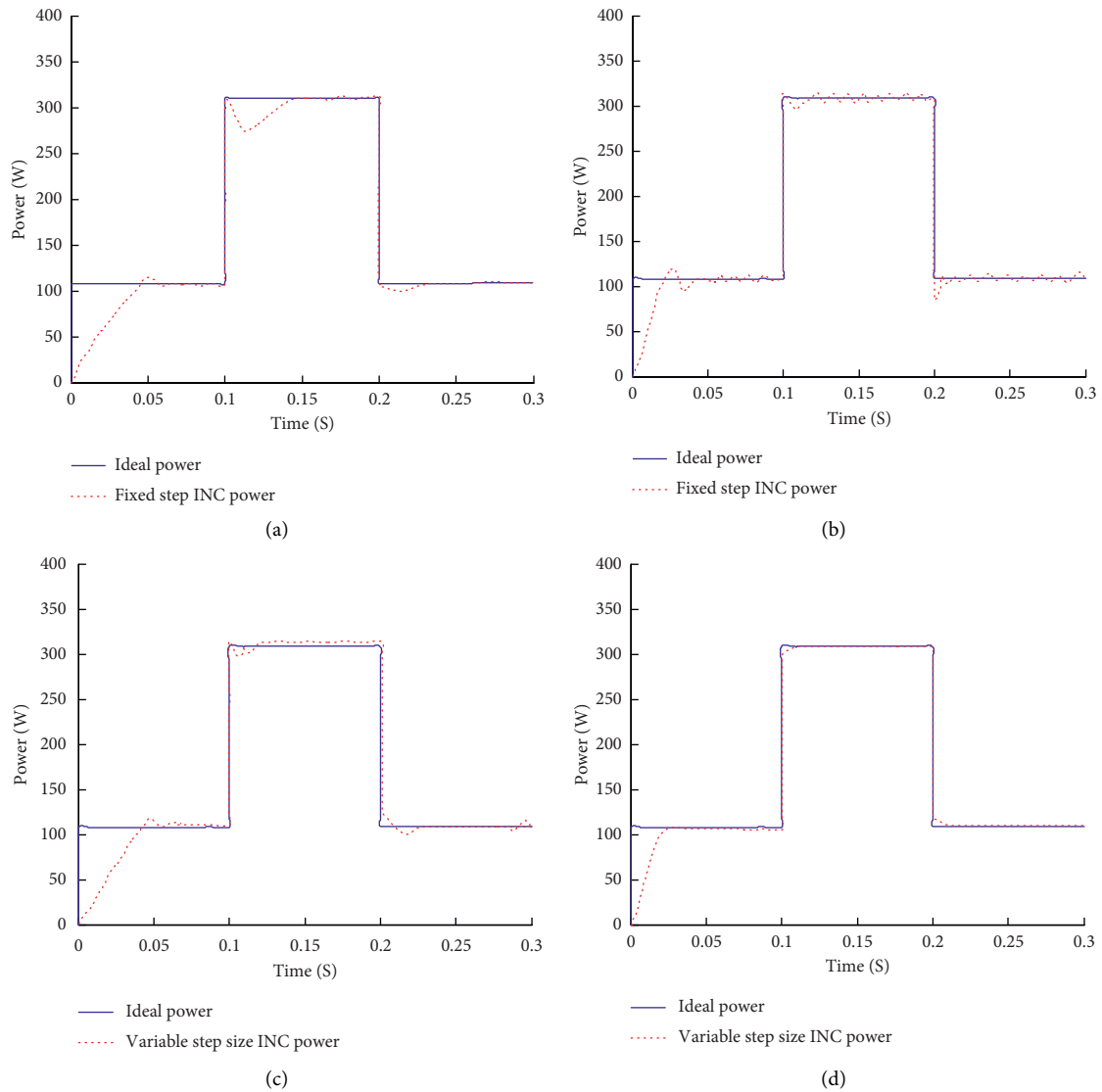


FIGURE 7: Comparison of tracking performance of algorithms. (a) Fixed step size INC, $\Delta U = 0.1$. (b) Fixed step size INC, $\Delta U = 0.5$. (c) Reference [13] variable step size INC. (d) Variable step size INC in this paper.

12.1 ms, respectively, and the average output power of the system is about 316.4 W when the light intensity is 1000 W/m². Compared with the fixed step size conductance increment method or the variable step size conductance increment method in reference [13], the tracking speed and steady-state accuracy of the system are greatly improved. This is mainly because the step size of this algorithm changes continuously according to the hyperbolic tangent form, which makes the algorithm really achieve fast and adaptive tracking of the actual maximum power point, so the performance of the algorithm is the best.

In order to compare the advantages and disadvantages of the algorithm in this paper and the algorithm in reference [13], the change of the step size of the algorithm with the change of illumination is given, as shown in Figure 8. It is obvious that no matter the light intensity suddenly increases or decreases, the step size of the algorithm in reference [13] is messy, sometimes large and sometimes small, and does not

change continuously in one direction, indicating that the adjustment is too large in the process of adjustment and even after the system output is stable, and sometimes the step size is not zero. In this algorithm, when the illumination suddenly increases and decreases, the step size changes in the same trend and adjusts rapidly, and the step size is kept at 0 after the system output power is stable, which realizes the maximum power point tracking control very well.

Algorithm consistency is also an important index to evaluate the performance of the algorithm. Because, when the above simulation conditions remain unchanged, 20 experiments are repeated, and the average value of the experiment is taken as the final result, as shown in Table 3.

As can be seen from the results in Table 3, the consistency of the three algorithms is good. When the light intensity changes, there is little difference in the results of repeated experiments, which is also the advantage of the conductance increment method. At the same time, it is

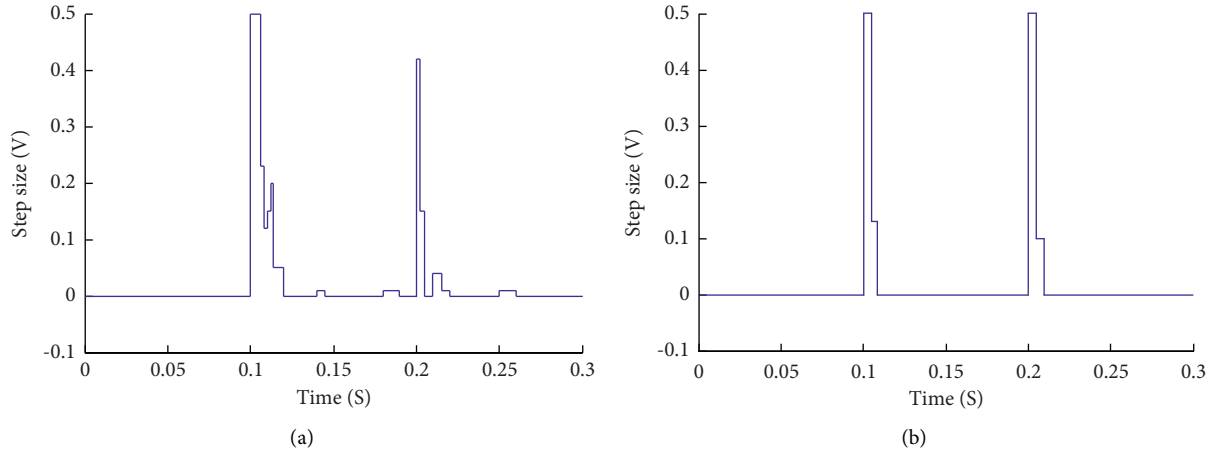


FIGURE 8: Comparison of algorithm step size. (a) Reference [13] the change of algorithm step size. (b) The change of algorithm step size in this paper.

TABLE 3: Comparison of simulation experiment data.

MPPT	Step size	System response time/ms			System steady-state error	
		Start	A sudden increase in light intensity	The light intensity drops suddenly	The light intensity is 400 W/m ²	The light intensity is 1000 W/m ² (%)
Fixed step size INC	$\Delta U = 0.1$	61.2	46.8	34.5	4.2%	0.51
	$\Delta U = 0.5$	24.3	24.5	13.7	4.91%	1.36
Reference [13] algorithm	$\Delta U_{\max} = 0.5$	32.2	22.5	22.8	1.38%	0.47
Algorithm in this paper	$\Delta U_{\max} = 0.5$	23.4	12.7	12.4	0.26%	0.16

further proved that the overall performance of this algorithm is obviously better than the fixed conductance increment method and reference [13] algorithm.

5. Conclusion

This paper focuses on the maximum power point tracking control of photovoltaic-thermoelectric power generation system. In view of the shortcomings of fixed step size selection in traditional conductance increment method, an adaptive step size increment method with gradual step size in hyperbolic tangent form is proposed. According to the simulation framework established by the mathematical model of photovoltaic-thermoelectric power generation system, the simulation experiment is carried out by MATLAB/Simulink software. The simulation results show that the hyperbolic tangent step size change law adopted in this paper can make the step size change quickly and adaptively, so that the output of the system can quickly track the maximum power point. When the light intensity changes sharply, the start-up time of the system can be effectively reduced, the system can quickly track the maximum power point in 15 ms, and the steady-state error is less than 0.3%. A good balance is achieved between the dynamic tracking speed and steady-state accuracy of the system, and the overall performance of the system is better. In addition, the algorithm proposed in this paper has the advantages of

simple principle and low hardware consumption, so it is very suitable to be implemented on DSP, FPGA, and other hardware, and can be quickly applied in practice.

Data Availability

The authors confirm that the data supporting the findings of this study are included within the article.

Conflicts of Interest

The authors declare that they have no conflicts of interest.

Acknowledgments

This work was supported by the Young academic backbone Project (GG2018004) of Mudanjiang normal University. This work was supported by the Project of Education Department of Heilongjiang Province (1452MSYYB009).

References

- [1] X. Liu, S. Guo, Z. Chang, Y. Peng, J. Hou, and Y. Li, "Research on the performance of a composite parabolic concentrating light-thermal photoelectric coupling energy supply device[J]," *Acta Solar Energy*, vol. 42, no. 07, pp. 262–268, 2021.
- [2] Q. Liu, C. Yan, D. Qian, X. He, and Y. Dou, "Simulation research on thermoelectric power generation performance

- based on dish concentrator[J],” *Power Technology*, vol. 45, no. 07, pp. 928–931, 2021.
- [3] Y. Vorobiev, J. González-Hernández, P. Vorobiev, and L. Bulat, “Thermal-photovoltaic solar hybrid system for efficient solar energy conversion,” *Solar Energy*, vol. 80, no. 2, pp. 170–176, 2006.
- [4] A. F. Mirza, Q. Ling, M. Y. Javed, and M. Mansoor, “Novel MPPT techniques for photovoltaic systems under uniform irradiance and Partial shading,” *Solar Energy*, vol. 184, pp. 628–648, 2019.
- [5] N. Femia, C. Petrone, G. Spagnuolo, and M. Vitelli, “Optimization of perturb and observe maximum power point tracking method[J],” *IEEE Transactions on Power Electronics*, vol. 20, no. 4, pp. 963–973, 2000.
- [6] F. Liu, S. Duan, F. Liu, B. Liu, and Y. Kang, “A variable step size INC MPPT method for PV systems[J],” *IEEE Transactions on Industrial Electronics*, vol. 55, no. 7, pp. 2622–2628, 2008.
- [7] Y. Zhao, L. Hong, L. Liu, and X. Gao, “The MPPT control method by using BP Neural Networks in PV generating system[C],” in *Proceedings of the 2011 2nd International Conference on Network Engineering and Computer Science*, vol. 9, pp. 482–487, Xi’an, China, 23–25 August 2012.
- [8] S. Xu, Y. Jin, and Q. Zhang, “Improved quantum-particle swarm optimization with global criterion[J],” *Systems Engineering and Electronics*, vol. 40, no. 9, pp. 2131–2137, 2018, (in Chinese with English abstract).
- [9] C. Lu, “Simulation study of MPPT control strategy based on an improved conductance increment method[J],” *Information & Technology*, vol. 3, pp. 111–115, 2019, (in Chinese with English abstract).
- [10] X. Zhai, H. Du, J. Liu, D. Ma, and C. Zhang, “Two-stage maximum power point tracking control based on particle swarm optimization and conductance increment method[J],” *Infrared and Laser Engineering*, vol. 45, no. 6, pp. 190–195, 2016, (in Chinese with English abstract).
- [11] J. Liu, X. Han, and P. Zhang, “Application of an improved variable step size conductance increment method in photovoltaic MPPT[J],” *Electrical Applications*, vol. 7, pp. 23–27, 2014.
- [12] D. Zhou and Y. Chen, “Maximum power point tracking strategy based on improved variable step size conductance increment method[J],” *Grid Technology*, vol. 39, no. 6, pp. 1491–1498, 2015, (in Chinese with English abstract).
- [13] L. Wang, F. Guanghuan, X. Zhang, S. Sun, and X. Li, “Design and performance test of concentrating solar photovoltaic/thermoelectric hybrid power generation system[J],” *Transactions of the Chinese Society of Agricultural Engineering*, vol. 34, no. 15, pp. 230–238, 2018, (in Chinese with English abstract).
- [14] J. Zhang, *Performance Analysis and Energy Matching Mechanism of the Photovoltaic-Thermoelectric Hybrid System[D]*, Nanjing University of Aeronautics and Astronautics, Nanjing, (in Chinese with English abstract), 2018.
- [15] J. Hou, Z. Song, H. F. Hofmann, and J. Sun, “Control strategy for battery/flywheel hybrid energy storage in electric ship-board microgrids,” *IEEE Transactions on Industrial Informatics*, vol. 17, no. 2, pp. 1089–1099, 2021.
- [16] R. Buckreus, R. Aksu, M. Kisacikoglu, M. Yavuz, and B. Balasubramanian, “Optimization of multi-port DC fast charging stations operating with power cap policy,” *IEEE Transactions on Transportation Electrification*, vol. 7, no. 4, pp. 2402–2413, 2021.
- [17] Z. Li, Y. Zhang, L. Wang, X. Jia, and Y. Zhang, “Study of photovoltaic multimodal maximum power point tracking based on improved quantum particle swarm optimization[J],” *Acta Energetica Solaris Sinica*, vol. 42, no. 5, pp. 221–229, 2021, (in Chinese with English abstract).
- [18] Z. Huang, Z. Xu, and L. Huang, “Development of double photoelectric solar tracking controller for photovoltaic-thermal integration device[J],” *Transactions of the Chinese Society of Agricultural Engineering*, vol. 37, no. 8, pp. 236–241, 2021, (in Chinese with English abstract).
- [19] H. Najafi and K. A. Woodbury, “Modeling and analysis of a combined photovoltaic-thermoelectric power generation system[J],” *Journal of Solar Energy Engineering*, vol. 135, no. 031013, pp. 1–8, 2013.